

Far Infrared Transmission through Superconducting Films*

D. M. GINSBERG† AND M. TINKHAM

Department of Physics, University of California, Berkeley, California

(Received December 30, 1959)

The far infrared transmission through films of superconducting and normal lead, tin, indium, and mercury has been measured in the wavelength region between 0.1 and 1.1 mm. The transmission data have been analyzed to find the ratio of the complex conductivity in the superconducting state to that in the normal state, as a function of frequency. The width of the energy gap at 0°K may be estimated from the frequency of the extrapolated cutoff of the real part, $\sigma_1(\omega)$, of the superconducting conductivity. The values so obtained are 4.0 ± 0.5 , 3.3 ± 0.2 , and $3.9 \pm 0.3kT_c$ for lead, tin, and indium, respectively. These values are in good agreement with those obtained in other experiments on bulk samples. The frequency dependence of $\sigma_1(\omega)/\sigma_N$ is in qualitative agreement with the results of a calculation by Mattis and Bardeen based on the theory of Bardeen, Cooper, and Schrieffer, except for an unexpected hump in $\sigma_1(\omega)$ for lead and (tentatively) mercury at low frequencies. This hump may be due to the production of collective excitations or an anisotropy in the energy gap. It has also been found that a magnetic field as high as 8000 gauss applied in the plane of a lead film about 12 Å thick has only a very small effect on the electromagnetic properties of the film. This is not surprising, in view of the results of the microwave experiments of Pippard and of Spiewak.

I. INTRODUCTION

IT is now well accepted, on both experimental¹ and theoretical² grounds, that the phenomenon of superconductivity is associated with an energy gap in the density of electronic states of a metal. The response of a superconductor to incident photons with an energy in the region of the gap width was first experimentally investigated by Glover and Tinkham.³ Their experiment consisted of measuring the transmission of far infrared radiation through thin films of normal and superconducting lead and tin. More recently, Richards and Tinkham^{4,5} have measured the reflection of radiation in the same spectral region from the surfaces of bulk samples of superconducting metals. In the same line of investigation, Biondi and Garfunkel⁶ have measured the absorption of microwave photons with energies in the region of the gap width in superconducting aluminum.

The experiments which we have performed are a further development of those of Glover and Tinkham. In principle, the present experiments are quite similar to the previous ones, but changes in optics and radiation detection have improved the accuracy of the results, and have permitted data to be obtained at considerably longer infrared wavelengths. We shall see that these developments have enabled us to obtain information which the older techniques could not have disclosed.

* Supported in part by the A. P. Sloan Foundation, the National Science Foundation, and the Office of Naval Research.

† Predoctoral National Science Foundation Fellow, now at the University of Illinois, Urbana, Illinois.

¹ M. A. Biondi, A. T. Forrester, M. P. Garfunkel, and C. B. Satterthwaite, *Revs. Modern Phys.* **30**, 1109 (1958).

² J. Bardeen, L. N. Cooper, and J. R. Schrieffer, *Phys. Rev.* **108**, 1175 (1957).

³ R. E. Glover, III, and M. Tinkham, *Phys. Rev.* **108**, 243 (1957).

⁴ P. L. Richards and M. Tinkham, *Phys. Rev. Letters* **1**, 318 (1958).

⁵ P. L. Richards and M. Tinkham, (to be published).

⁶ M. A. Biondi and M. P. Garfunkel, *Phys. Rev.* **116**, 853 (1959).

We have also investigated the effect of a magnetic field on the properties of lead films.

II. EXPERIMENTAL METHOD

A. Low-Temperature Techniques and Film Production

The Dewar used in these experiments is quite similar to that used in the experiments of Glover and Tinkham, but incorporates two main changes. One of these enables us to bring the radiation into and, when desired, out of the Dewar through stainless steel tubes, as is required for the new optical techniques. The other change in the Dewar enables us to move the film in or out of the radiation beam while the film is at a low temperature.

A schematic drawing of part of the Dewar appears in Fig. 1. The infrared radiation is brought into the Dewar through a stainless steel light pipe, which is $\frac{1}{2}$ in. in

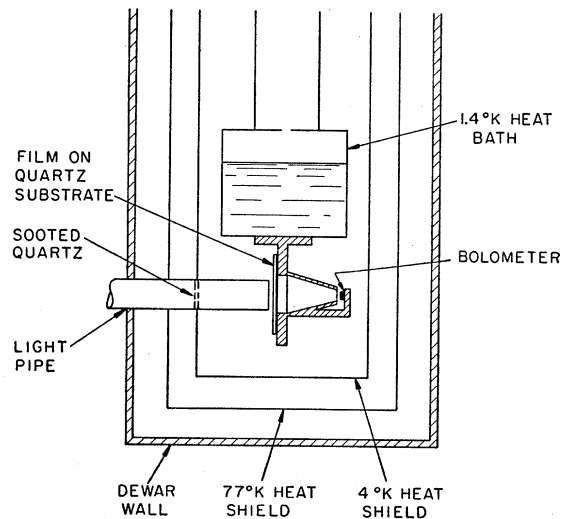


FIG. 1. Schematic drawing of Dewar.

diameter. During the film evaporation, this pipe is moved back from the substrate, but during the infrared measurements, the end of the pipe is about $\frac{1}{16}$ in. from the film. The thermal connection from the heat shields to the pipe is provided by flexible copper braids. A piece of sooted crystalline quartz glued in the cold end of the light pipe absorbs room temperature radiation before it can strike the film. This quartz completes the radiation shielding which encloses the film. In the pipe leading to the helium tank in Fig. 1 there is an orifice, $\frac{1}{8}$ in. in diameter, which reduces the loss of liquid helium due to superfluid creep. Pumping on the helium through this pipe permits us to obtain temperatures as low as 1.4°K. (The filling tube for the tank is not shown in the figure.)

The production of the film is similar to that in the previous work.³ The film is approximately 2 cm square, and is produced by the evaporation of the metal onto a clean crystalline quartz substrate at 77°K in a vacuum of about 10^{-5} mm of mercury. Two gold electrodes, evaporated onto the quartz before the film is deposited, permit the film resistance to be monitored during the evaporation, which requires about three seconds for completion. The film is kept in vacuum during the entire investigation. Before infrared work is begun, the film is annealed overnight at room temperature for lead, tin, and indium, and at 77°K for mercury. (Buckel and Hilsch⁷ have observed that mercury films anneal satisfactorily at this temperature.)

The substrate is a piece of *z* cut optically polished quartz of dimensions 1 in. × 1 in. × 0.080 in. It is attached, as is an identical piece of quartz with no film, to a copper sled (not shown in Fig. 1). The sled slides back and forth in a holder which is screwed to the helium tank, and which has a $\frac{5}{8}$ -in. diameter hole in it. The sled has two $\frac{1}{16}$ -in. diameter holes in it, one behind each piece of quartz. By sliding the copper sled back and forth, the infrared radiation reaching the detector through the hole in the holder can be made to pass either through the film or through the bare quartz. The sled is thermally tied to the small helium tank with a copper braid, soldered with a nonsuperconducting solder consisting of 83% cadmium and 17% zinc. The sliding motion is driven by two stainless steel wires, each 0.010 in. in diameter, which pass through small holes in the heat shields. These wires are attached to pieces of nylon string which in turn may be wound up on shafts to provide the motion. These shafts pass

through O-ring seals, and are turned manually from outside the Dewar. The wires are thermally anchored to the 77°K heat shield by flexible copper braids.

The sources and purities of the metals used to make the films are given in Table I.

B. Infrared Monochromator

The far-infrared monochromator used in this work was designed with the help of Richards, and is described elsewhere.⁵ The output radiation is chopped at 9 cps, and is of high purity. The purity was tested at various times by increasing the amount of radiation filtering and watching for an apparent change in the frequency dependence of the transmissivity of a superconducting film. The results of this testing indicate that at 900 microns only about 1% of the radiation lies significantly outside of our nominal bandwidth, e.g., at harmonic frequencies. For wavelengths shorter than 750 microns, the amount of energy outside of the estimated bandwidth was too small to be detected in these tests. The estimated bandwidth between half-power points is approximately 12% at all wavelengths.

C. Radiation Detection

The radiation is detected by means of a carbon resistance bolometer similar to that described by Boyle and Rodgers,⁸ but with evaporated indium electrodes. The bolometer is a slab, of dimensions $\frac{1}{8}$ in. × $\frac{1}{4}$ in. × $\frac{1}{60}$ in., cut from a 56 ohm, 2 watt Girard Hopkins radio resistor. Using GE 7031 glue, the bolometer is glued to a piece of Mylar, 0.0005 in. thick, which is in turn glued to a piece of metal which is at a temperature of about 1.4°K during the experiment. A brass cone is used to gather the light toward the bolometer, as shown in Fig. 1. A copper shield, not shown in the figure, completely encloses the bolometer to insure that any chopped radiation incident on the bolometer passes first through the film or the bare quartz. Using pure indium solder, electrical contact to the bolometer is made with number 38 Manganin wires. The bolometer current is provided by a 22 volt battery in series with a variable resistor, *S*, adjustable between 1 and 3 megohms for maximum signal-to-noise ratio. Under the usual conditions, the bolometer resistance is between 100 kohm and 200 kohm, and the bolometer signal is between 0.5 and 130 microvolts. The signal is capacitively coupled into the first stage of a conventional 9 cps lock-in amplifier. The output of the amplifier appears on a Varian chart recorder.

The signal-to-noise ratio of one of our bolometers was determined to be of the order of 50 times that of two different Golay cells, for a given amount of incident radiation. (These cells, which were used in the work of Glover and Tinkham, are said by the manufacturer, the Eppley Laboratories, to have an equivalent noise

TABLE I. Metal sources and purities.

Metal	Manufacturer	Stated Purity
Lead	Johnson, Matthey	0.99998
Tin	Johnson, Matthey	0.9999
Indium	Johnson, Matthey	0.994
Mercury	Quicksilver Products	Triple distilled

⁷ W. Buckel and R. Hilsch, *Z. Physik* **138**, 109 (1954).

⁸ W. S. Boyle and K. S. Rodgers, Jr., *J. Opt. Soc. Am.* **49**, 66 (1959).

input power of 6×10^{-11} watts in a bandwidth of 1 cps) One such bolometer was cycled between room temperature and 1.4°K many times during a period of six months, with no noticeable increase in noise or loss in sensitivity. The proximity of the bolometer to the film also helps in obtaining a high signal level.

The bolometer resistance is monitored continuously by a high-impedance null-balance circuit in parallel with the bolometer. This permits us to calibrate the bolometer sensitivity as a function of its resistance as follows. (This calibration is required to make certain corrections discussed later.) By varying the resistance S , the bolometer's current, and hence its temperature and resistance can be changed. For a given amount of infrared power incident on the bolometer, the signal is measured for various values of S . The signal size is then corrected for the variation in bolometer current and shunting due to changing S . In this way, we obtain the relation between bolometer sensitivity and resistance for a value of S which is constant, namely the value used during our infrared measurements. This method of determining the relation between bolometer resistance and sensitivity gives approximately the same results as those obtained by changing the bolometer resistance by altering the bath temperature or by sending additional current through the bolometer at a frequency of 100 kc/sec. This relation of sensitivity to resistance is approximately linear.

D. Method of Making the Measurements

The critical temperature, T_c , of a film is determined by slowly lowering the temperature by pumping on the helium bath while monitoring the film resistance. This remains approximately constant until the region of the superconducting transition is approached, and then decreases rapidly to zero. The critical temperature is taken to be that at which the film resistance is one-half of its low-temperature value in the normal state. In the case of lead films, temperatures above 4.2°K are required. They are obtained by operating with helium in only the outer tank of the Dewar and suitably balancing the heat input from a resistance heater against the cooling through the thermal contact between the two helium tanks. Temperatures above 4.2°K are measured by a carbon resistance thermometer calibrated below 4.2°K by using the 1958 helium vapor pressure scale, and calibrated at 7.175°K by using the superconducting transition of a 0.99998 pure lead wire.

All of the infrared measurements are made at the lowest obtainable temperature, about 1.4°K . The critical current at this temperature is determined by sending a gradually increasing current through the film and observing the magnitude of the current when the film resistance suddenly reappears. With reference to the values given below for the magnitude of the critical current, it should be noted that the width of the film transverse to the direction of current flow is 2 cm.

The infrared measurements are made as follows. With sufficient current passing through the film to hold it in the normal state, and with infrared radiation of a fixed wavelength entering the Dewar, the sliding mechanism described above is used to enable us to measure alternately the energy passing through the film and quartz and that passing through the bare quartz. This is done several times to average over noise and slight drifts in sensitivity, each measurement lasting for several times the time constant of the lock-in amplifier, (13 to 72 seconds.) In this way, it is found that the transmissivity, T_N , of the film in the normal state is independent of wavelength throughout our region of the spectrum.

In a similar manner, the wavelength dependence of the transmissivity, T_S , of the superconducting film is determined. In comparing T_N and T_S , the following facts must be taken into account. The amount of thermal radiation reaching the bolometer changes significantly when the film and quartz are replaced by the bare quartz. As a result, the bolometer temperature, and hence its operating point and sensitivity, change. Our calibration of bolometer resistance and sensitivity, described above, permits us to correct for this effect, since we monitor the bolometer resistance continuously. The correction on T_S or T_N is roughly a factor of two. The size of the correction depends only slightly on whether the film is superconducting or normal, the difference arising from the bolometer temperature rise because of the Joule heating due to the current in the normal film. As a result, the ratio T_S/T_N is altered by only about 5% by the correction. Because of the possibility of error in the correction factor, T_S or T_N can not separately be measured very accurately in this way, although their ratio can be. If we need an accurate measure of T_S or T_N individually, we use a bolometer in another Dewar, the radiation being brought out of the Dewar containing the film and then to the bolometer via metal light pipes. Under these circumstances, the bolometer is called an external detector, and its sensitivity is unaffected by the film's position, since there are thermal radiation filters between film and bolometer. Unfortunately, the use of the external detector decreases the signal obtainable so much as to prevent us from obtaining accurate data at long wavelengths, where the source intensity is low.

III. THE EXPERIMENTAL DATA AND THEIR ANALYSIS

A. Noninfrared Data

Table II summarizes some of the information concerning the films which we have examined. The symbols used have the following meanings. R_1 , R_2 , and R_3 are, respectively, the film resistances immediately after the film is made, after it is annealed, and after it is then cooled to about 1.4°K (and held in the normal state). These resistances have each been multiplied by a factor which yields the resistance the film would have

if it were square. (The film is rectangular, and almost square.) I_c is the critical current of the film at about 1.4°K. ΔT is the width of the superconducting transition, defined to be the temperature interval in which the film's resistance decreases from 80% to 20% of the normal state low-temperature resistance, as the temperature is lowered. T_c is the critical temperature, at which the film resistance is one half its normal state low-temperature value. T/T_c is the reduced temperature at which the infrared data were obtained. We have assumed all our lead films to have the same critical temperature, 7.06°K, as Pb3 and another lead film not included in Table II. The thickness of a film can be estimated^{8,9} very roughly by using Matthiessen's rule¹⁰ and the values of R_2 and R_3 . In this way one finds the thickness to range between about 5 and 15 Å. We do not need to know the thickness to interpret our results, so a more precise determination is unnecessary.

The resistances in Table II are accurate to within 0.5 ohm, I_c to within 2%, ΔT to within 0.002°K, T_c to within 0.08°K except for lead, for which T_c has a maximum error of 0.5°K. Sn2 was produced by partially oxidizing Sn1 at room temperature to examine the effect of this oxidation. Somewhat nonideal behavior of these films is indicated by the displacement, up to 0.4°K, of T_c from the value for bulk samples, and by the comparatively large values of ΔT . The displacement of T_c from the value for bulk samples is largest for the mercury films. (T_c is 4.15°K for bulk mercury.¹¹) The reason for this might be that the films are partially or totally composed of β mercury,¹² a crystallographic modification with a critical temperature of 3.94°K. Buckel and Hilsch⁷ also have observed

TABLE II. Noninfrared properties of the films.

Film	R_1 ohms	R_2 ohms	R_3 ohms	I_c ma	ΔT °K	T_c °K	T/T_c
Pb1	376	440	254	106	0.212
Pb2	470	615	305	155	0.200
Pb3	269	425	197	460	...	7.06	0.198
Pb4	219	260	115	97
Pb5	292	220
Sn1	329	287	152	56	0.060	3.88	0.365
Sn2	...	420	230	36	0.120	3.90	0.350
Sn3	222	107
Sn4	244	302	168
In1	231	349	252	38	0.035	3.88	0.336
In2	183	274	193
In3	191	269	187
Hg1	206	178	84	36	0.002	3.79	0.343
Hg2	313	269	127	52	0.009	3.85	0.405
Hg3	229	154	76	38	0.004	3.75	0.328
Hg4	191	165	78
Hg5	208	165	84
Hg6	314	288	120

⁹ E. T. S. Appleyard and J. R. Bristow, Proc. Roy. Soc. (London) **A172**, 530 (1939).

¹⁰ A. H. Wilson, *The Theory of Metals* (Cambridge University Press, London, 1954).

¹¹ L. D. Jennings and C. A. Swenson, Phys. Rev. **112**, 31 (1958).

¹² J. E. Schirber and C. A. Swenson, Phys. Rev. Letters **2**, 296 (1959).

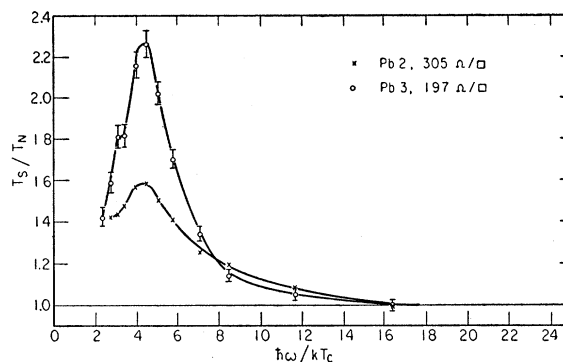


FIG. 2. Transmission characteristics of Pb2 and Pb3.

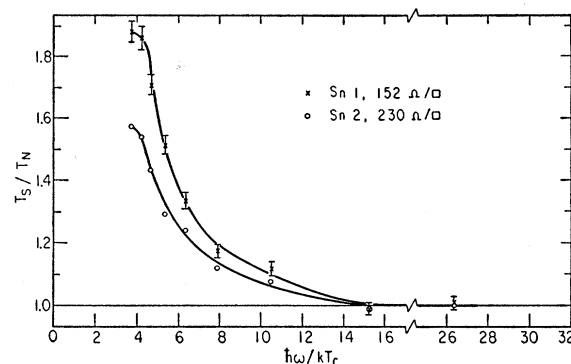


FIG. 3. Transmission characteristics of Sn1 and Sn2.

mercury films to possess a low critical temperature, about 3.85°K. A visual examination of our lead, tin, and indium films disclosed no lack of uniformity. The mercury films evaporated when warmed to room temperature, and so could not be visually examined.

B. Infrared Data

The frequency dependence of the ratio of the transmission, T_S , through the superconducting film to that, T_N , through the normal film, for seven of our films is shown in Figs. 2 through 5. As explained below, we expect this ratio to be correct to within $\pm 3\%$. The most complete curves are those for Pb2 and Pb3. For the other metals, the critical temperatures are lower, and we can not reach such low reduced frequencies as for lead. (By the reduced frequency we mean $\hbar\omega/kT_c$, where k is the Boltzmann constant.) To avoid illegibility, maximum errors are indicated for only some of the points in the figures.

It is quite evident that the general shapes of all the transmission curves are quite similar. At high frequencies, the transmission ratio approaches unity. As the frequency is lowered, this ratio rises to a maximum and then falls. This kind of behavior would be predicted by nearly any energy gap model. In particular, it is predicted by the theory of Bardeen, Cooper, and Schrieffer,² hereafter referred to as BCS. The fact that the maximum in each curve occurs at approximately

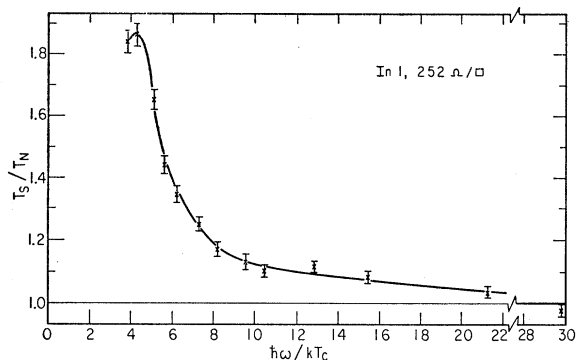


FIG. 4. Transmission characteristics of In1.

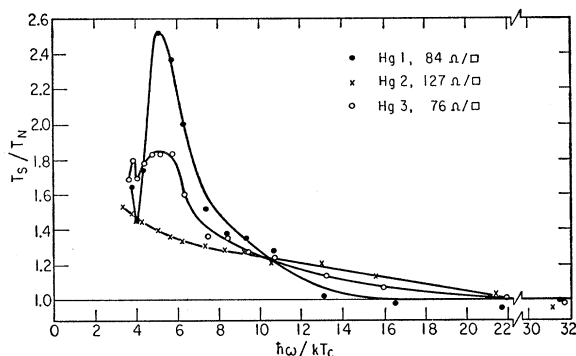


FIG. 5. Transmission characteristics of Hg1, Hg2, and Hg3.

the same reduced frequency suggests immediately that the energy gap is approximately proportional to the critical temperature, as predicted by BCS.

C. Inference of Conductivity Curves from the Infrared Data

We wish to use the transmission data just presented in order to calculate the conductivity ratio,

$$[\sigma_1(\omega) + i\sigma_2(\omega)]/\sigma_N,$$

where $\sigma_1 + i\sigma_2$ is the complex superconducting conductivity and σ_N is the normal-state conductivity. The latter is real and independent of frequency in this region of the spectrum, as is shown by the fact that T_N is found to be frequency-independent. (Note that we have changed the convention of reference 3, where $\sigma = \sigma_1 - i\sigma_2$. The present convention corresponds to an $e^{-i\omega t}$ time dependence, as is usual in quantum theory.) Since the real and the imaginary parts of the conductivity are related by the Kramers-Kronig relations,³ we need only calculate one of them. We calculate $\sigma_1(\omega)/\sigma_N$. In order to calculate this from the transmission ratio, we use Eq. (A-2) of reference 3, which is hereafter referred to as GT. In the derivation of this equation it is assumed that one can average over standing waves in the quartz substrate. This is not exactly true, since the radiation bandwidth is finite. The

maximum error from this averaging has been estimated¹³ to be equivalent to an error in the transmission ratio of $\pm 0.2\%$ for all films except the unusually conductive one Pb3, for which the error may be as large as $\pm 0.5\%$ for $\hbar\omega/kT_c > 4$. For frequencies above the maximum in the curve of the transmission ratio, it turns out that we may ignore all reflections in the substrate and use Eq. (A-4) of GT without appreciable error.

We can calculate σ_1/σ_N from T_S/T_N only if we first know σ_2/σ_N . In order to circumvent this difficulty, we have two aids. One is provided by the Kramers-Kronig (K-K) relations,³ and the other by a conductivity sum rule pointed out by Ferrell and Glover,¹⁴ and discussed further by Tinkham and Ferrell.¹⁵ According to this rule,

$$\int_0^\infty \sigma_1(\omega) d\omega = \int_0^\infty \sigma_N(\omega) d\omega, \quad (1)$$

where σ_N is now the real part of the normal conductivity. Since this is independent of frequency in the frequency range in which σ_1 differs appreciably from σ_N , Eq. (1) has as a consequence the fact that any area under the σ_1/σ_N curve removed by the appearance of the gap appears in a delta function in σ_1 at zero frequency. The K-K transform, σ_2^A , of this δ function is inversely proportional to the frequency. (See GT or reference 15 for a more complete description. In calling this term σ_2^A we follow the notation of reference 15, reserving σ_2^L for the London value of σ_2^A which arises when the entire sum rule area appears in the δ function.) Adding σ_2' , the K-K transform of that part of σ_1 lying above zero frequency, to σ_2^A , gives $\sigma_2(\omega)$.

Our method of calculating σ_1/σ_N is, then, as follows. We assume that a simple energy gap model is useful as a first approximation. Such a model predicts $\sigma_2(\omega)/\sigma_N$ to be small for $\omega > \omega_g$, where $\hbar\omega_g$ is the gap width. Therefore we first assume that σ_2 is negligibly small for frequencies higher than that corresponding to the maximum in T_S/T_N . The function σ_1/σ_N is then cal-

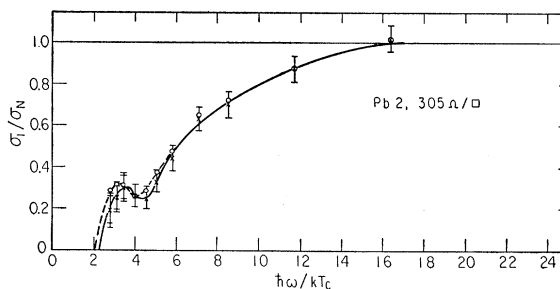


FIG. 6. Frequency dependence of σ_1/σ_N for Pb2. The solid curve is calculated using the measured film resistance, the broken curve using the calculated value. (See text.)

¹³ D. M. Ginsberg, Ph.D. thesis, University of California (unpublished).

¹⁴ R. A. Ferrell and R. E. Glover, III, Phys. Rev. **109**, 1398 (1958).

¹⁵ M. Tinkham and R. A. Ferrell, Phys. Rev. Letters **2**, 331 (1959).

culated on this basis for frequencies above the maximum in the transmission ratio, and it is extrapolated smoothly to zero, as suggested by the simple energy gap model. Then we calculate σ_2^A from the sum rule, and we numerically calculate σ_2' from the K-K relations. Adding these together, we obtain our first approximation for σ_2 . This we use with the transmission ratios to calculate our second approximation for σ_1 . This always is found to agree with the first approximation, for $\hbar\omega/kT_c \gtrsim 6$. This cycle of operations is repeated until it converges for all frequencies, which happens after the cycle is repeated about twice. We finish with a curve for σ_1/σ_N which is consistent with the conductivity sum rule, and which accounts for the measured values of T_S/T_N when combined with the $\sigma_2(\omega)/\sigma_N$ curve which is its Kramers-Kronig transform.

There is one complication in performing this calculation, which we now describe. We must know the normal film resistance in order to use the equations to calculate the conductivity function. We have measured this at dc, but we do not know that it is exactly the same for our infrared frequencies, which lie between 3×10^{11} and 3×10^{12} cps. In fact, using an external detector (see above), we have shown that our lead, tin, and indium films are slightly more opaque in the normal state at infrared frequencies than the dc resistance would indicate. From the infrared transmissivity we can calculate a resistance value. We can compare this calculated resistance, R_{calc} , with the measured resistance, R_{meas} . In this way, it is found that at low temperatures $R_{\text{meas}}/R_{\text{calc}}$ is about 1.11 for lead films, 1.01 for tin films, and 1.26 for indium films. This ratio of resistances is found to be about the same for all films of a given metal at a given temperature, but it increases slightly with increasing temperature. In the case of mercury, however, this is not true; the ratio of resistances varies greatly from one film to another. For all of the films this ratio is independent of frequency in our infrared region of the spectrum. The film resistance is also found by measurement to be constant between dc and 100 kc/sec. (The films used in making these observations were all those in Table II for which transmission curves have not been presented because of the relatively low sensitivity of the external detec-

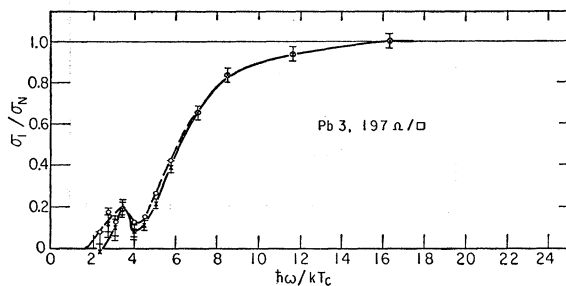


FIG. 7. Frequency dependence of σ_1/σ_N for Pb3. The solid curve is calculated using the measured film resistance, the broken curve using the calculated value. (See text.)

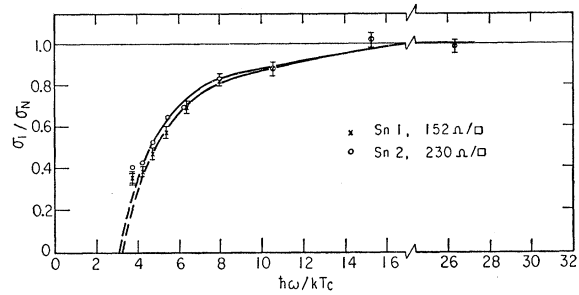


FIG. 8. Frequency dependence of σ_1/σ_N for Sn1 and Sn2.

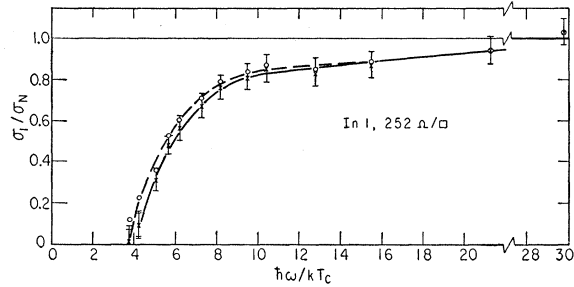


FIG. 9. Frequency dependence of σ_1/σ_N for In1. The solid curve is calculated using the measured film resistance, the broken curve using the calculated value. (See text.)

tor. An exception is Pb1, which we shall discuss later.) It may be that there are imperfections in the film which become short circuited by capacitive effects in the frequency range between 10^5 and 10^{11} cps. In the case of the mercury films, variations in the thickness of a given film from one region of the film to another may also be important in explaining the observed phenomena. (Other investigations¹⁶ have also indicated that mercury tends to form uneven deposits on quartz.)

In calculating the conductivity ratio from the transmission ratio, we can either use the measured film resistance R_{meas} or the calculated value R_{calc} . In Figs. 6 through 9, which show the calculated conductivity ratios, the results of the latter method are indicated by dashed lines. In the case of tin, the two methods give nearly the same answer, since $R_{\text{calc}}/R_{\text{meas}}$ is approximately unity. Since the properties of the mercury films were so erratic, we have made no attempt to calculate the conductivity ratio for them. Hence we confine our remarks on mercury to observations which can be made directly from the features of the transmission curves.

D. Discussion of Errors

The greatest single source of error is random noise on the signal. This error is less than 1.5% at a 90% confidence level. Another possible source of error in this experiment comes from the large aperture of our f/1.5 infrared monochromator. Radiation is incident on the film at angles up to 18.5° from the normal. One cannot

¹⁶ R. E. Glover, III (private communication).

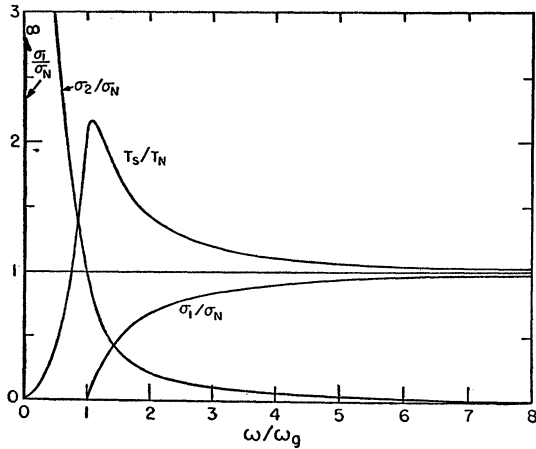


FIG. 10. Frequency dependence of σ_1/σ_N , σ_2/σ_N , and T_S/T_N according to the calculation of Mattis and Bardeen. The transmission curve is for a film resistance $377/(n+1)$ ohms per square, where n is the refractive index of the substrate.

calculate the effect of this non-normal incidence with complete certainty without a detailed knowledge of the film properties. However, if we make the usual assumption that currents in a direction normal to the film surface are completely negligible, then it can be calculated¹³ that the finite focal ratio affects T_S or T_N by less than 2% and T_S/T_N by less than 0.2%. We shall, however, mention shortly the possibility of resonant normal oscillations in the film which might make the non-normal incidence important. Another possible source of error comes from standing waves in the quartz substrate. As has already been mentioned, this affects the transmission ratio by less than 0.5% in all cases.

In the data shown in Figs. 6 through 12, there are two possible errors indicated. The inner error sign is the result of a total $\pm 3\%$ possible error in T_S/T_N from the sources mentioned above. The outer error sign results from adding on the effect of a $\pm 3\%$ possible error in A , the area removed by the gap. This error is a secondary consequence of the previously mentioned errors. This additional error is important only for the low-frequency points, as indicated in the figures. The reason for separating the errors into two parts in this way is that an error in A would affect neighboring points similarly, and so would not change the shape of the curve very much.

IV. COMPARISON OF CONDUCTIVITY CURVES WITH THEORY AND WITH OTHER EXPERIMENTS

A. Comparison with the BCS Theory

Mattis and Bardeen¹⁷ have calculated σ_1/σ_N from the BCS theory. This calculation is expected to apply when the characteristic distance for variation of the field in the samples in the normal state is small compared with the mean free path l , and in the supercon-

ducting state is small compared with the coherence length¹⁸ ξ_0 . Since ξ_0 is of the order of 2000 Å, this condition is well satisfied in these thin films, and reasonably well satisfied in the skin effect in pure normal metals. The theoretical frequency dependence of σ_1/σ_N is shown in Fig. 10. It is approximately independent of temperature for $T/T_c < \frac{1}{3}$. We see immediately that this dependence shows a remarkable qualitative agreement with that which we have observed, as shown in Figs. 6 through 9.

There are three quantitative differences, however, between our curves and the theoretical predictions. In the first place, our data indicate an unexpected hump in σ_1/σ_N for lead. The mercury transmission data of Fig. 5 also would tend to indicate such a hump. Later we shall consider possible reasons for this hump.

The second disagreement between our conductivity curves and the predictions of the theory, which occurs for the two tin films, is the failure of σ_1/σ_N to fall to zero rapidly as $\hbar\omega/kT_c$ decreases below the nominal gap frequency. This seems to indicate a genuine low frequency tail on the conductivity curve even at low temperatures. Any explanation based on the finite temperature of the film is unlikely to be correct, because the indium film In1 at approximately the same reduced temperature has a conductivity curve which apparently has no such tail, but rather gives the sharp cutoff at the gap predicted by the theory. Any tail might be due to the nonideal nature of the films. This conjecture is supported by the fact that Sn2, which was produced by partially oxidizing Sn1 and might therefore be expected to be less ideal than Sn1, has a larger tail. In Fig. 8, σ_1/σ_N is extrapolated to zero ignoring the lowest-frequency points. Some extrapolation was needed to allow σ_2/σ_N to be calculated by the

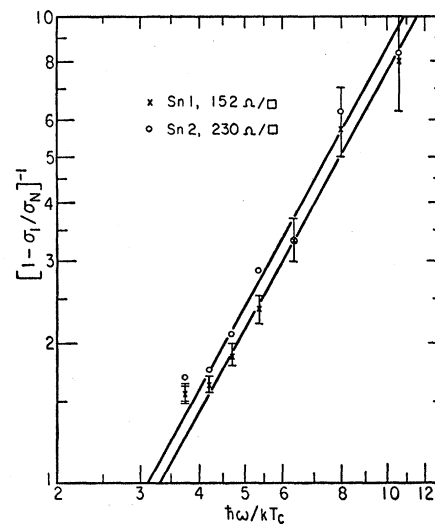


FIG. 11. Logarithmic plot of the frequency dependence of $(1 - \sigma_1/\sigma_N)^{-1}$ for Sn1 and Sn2.

¹⁷ D. C. Mattis and J. Bardeen, Phys. Rev. **111**, 412 (1958).

¹⁸ A. B. Pippard, Proc. Roy. Soc. (London) **A216**, 547 (1953).

procedure described above. Changing the extrapolation would not seriously change the results of our calculation of σ_1/σ_N in the region where we have data, because σ_2/σ_N has very little effect on T_S/T_N at such high reduced frequencies.

The third disagreement between our results and the theoretical predictions is that σ_1/σ_N seems to approach unity somewhat more rapidly than predicted, as $\hbar\omega/kT_c$ increases well above the gap. This is more clearly brought out by Figs. 11 and 12. In these figures we plot $\log (1-\sigma_1/\sigma_N)^{-1}$ against $\log \hbar\omega/kT_c$. According to the BCS theory, this plot should be an almost straight line, with a slope, n , of approximately 1.61 in the range $1 < \omega/\omega_g < 2.5$, where $\hbar\omega_g$ is the gap width. It is in this range that we can most accurately compare theory with experiment. The figures show that we do indeed obtain plots which are approximately linear, for tin and indium. This is not true for lead, for reasons which are probably connected with the hump in σ_1/σ_N for lead. Our values for the slope n are given in Table III. Their excess above 1.61 is a measure of the increased steepness of the rise in σ_1/σ_N .

Table III also gives our values for “ a ” and for “ a^* ”, which are defined as follows in terms of σ_2^A .

$$\sigma_2^A/\sigma_N = (1/a)(kT_c/\hbar\omega) = (2A/\pi)(kT_c/\hbar\omega).$$

“ a^* ” is the value of “ a ” computed from the dashed curves of Figs. 6 through 9. (The constant A is defined above as the area removed from the σ_1/σ_N curve by the gap.)

It is seen from Table III that, according to our data, n is greater than the value 1.61 predicted by BCS. Correspondingly, A is smaller, and “ a ” is larger than 0.18, the BCS value. Our value for “ a ” should also be compared with the value 0.21 ± 0.05 which was indi-

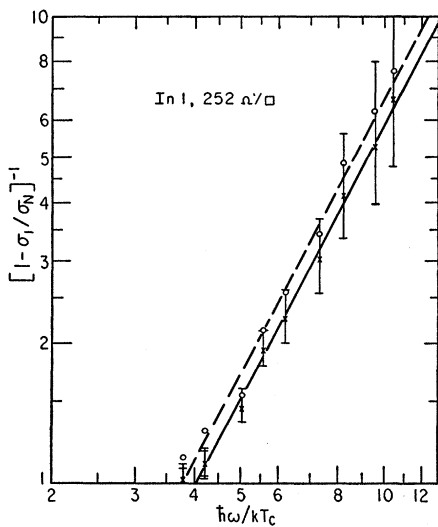


FIG. 12. Logarithmic plot of the frequency dependence of $(1-\sigma_1/\sigma_N)^{-1}$ for In1. The solid curve is calculated using the measured film resistance, the broken curve using the calculated value. (See text.)

TABLE III. Infrared properties of the superconducting films.

Film	n	a	a^*
Pb2	...	0.232	0.241
Pb3	...	0.231	0.242
Sn1	1.83	0.258	0.258
Sn2	1.83	0.270	0.270
In1	1.97	0.193	0.210

cated by the infrared data of GT for lead and tin films,¹⁴ and with the value 0.15 which was found by Faber and Pippard¹⁹ from their microwave work on aluminum and tin at a frequency of 1200 Mc/sec. All of these values seem to be in reasonable agreement, considering differences in experimental geometries and materials, and considering the simplified nature of the theory.

In concluding this section, it might be well to call attention to the fact that the shape of our conductivity curves should be compared with those derived from experiments on bulk samples only if the electromagnetic skin depth of these samples is small compared with ξ_0 and with the electron mean free path in the normal state. Otherwise the behavior of the bulk samples will involve a complicated average¹³ over various spatial Fourier components of the electromagnetic field.

B. Width of the Energy Gap

We can estimate the width of the energy gap from the extrapolated cutoff of σ_1/σ_N . For lead, this can be done from Figs. 6 and 7. For tin and indium, this is most easily done from Figs. 11 and 12. Our results are indicated in the last column of Table IV. In the Table, our values for the gap width are compared with those derived from thermal data and with other far-infrared data. The analysis of the thermal data has been given by Goodman.²⁰ He has used three methods to calculate the gap width from the data. Method A consists of a detailed fitting of the specific heat over a wide temperature range to a BCS expression in terms of the gap width at 0°K. Method B consists in fitting low-temperature data to an exponential dependence of specific heat on the inverse of the temperature. Method C relies on an expression given by BCS for the width of the gap at 0°K in terms of the critical field and the electronic

TABLE IV. Values for the reduced gap width, $\hbar\omega_g/kT_c$.

Metal	Goodman			Richards and Tinkham	
	A	B	C	This work	This work
Lead	3.9	4.1	4.0 ± 0.5
Tin	3.3	3.6	3.6	3.6	3.3 ± 0.2
Indium	...	3.9	3.5	4.1	3.9 ± 0.3

¹⁹ T. E. Faber and A. B. Pippard, Proc. Roy. Soc. (London) **A231**, 336 (1955).

²⁰ B. B. Goodman, Superconductivity Conference, Cambridge, England 1959 (unpublished).

specific heat in the normal state. The gap width values obtained by these methods have been divided by kT_c , where T_c is the experimentally determined critical temperature, to obtain values for the reduced gap width. The fourth column of the Table gives values for the reduced gap width as determined for bulk samples by Richards and Tinkham.⁵ For the latter values and for our values, the gap width values at 0°K have been calculated from the experimental data by assuming that the temperature dependence of the gap is given correctly by BCS. The adjustment in the gap width involved in this procedure is completely negligible in the case of lead, and is only 1% for tin and indium. For lead, we take the gap width to be given by the frequency at which it is estimated that σ_1/σ_N would cutoff if the subsidiary hump in the curve did not exist.

It is evident that our values for the gap width are in remarkable accord with those determined by these other experiments, considering the extremely microscopic size of our samples. This is perhaps one of the most interesting results in this kind of investigation of thin films.

Ultrasonic experiments²¹ on tin have disclosed a rather large apparent anisotropy in the energy gap which may also be present in other superconductors. It is evident that the thermal data must indicate some sort of average gap width. This may also be true in the infrared experiments. However, Anderson²² has suggested that any anisotropy of the gap will be averaged out in samples in which the electronic scattering frequency exceeds the gap frequency, as it does by a wide margin in these films. Similarly, scattering of electrons in the surface layers of a bulk sample might destroy any evidence of gap anisotropy which the experiments of Richards and Tinkham otherwise might have indicated.

C. Structure on the Absorption Edge

The available explanations for the observed hump in the σ_1/σ_N curve for lead (and presumably mercury) fall into two general categories: single particle and collective excitations. The most straightforward is the former. One simply presumes that the gap is anisotropic, i.e., that the minimum energy for the creation of an excitation depends on where it is created on the Fermi surface.²³ Since the Fermi surfaces of the metals under consideration here (lead, tin, and mercury) are expected to consist of several pieces lying in different Brillouin zones, it would not be surprising if the gap had distinct values on different parts of the surface. Given suitable selection rules, a small piece of surface with a smaller gap might give rise to the observed hump of absorption at frequencies below that where

the main absorption sets in. The existence of a substantial number of states with a smaller gap would also give a natural explanation of the fact that the departure from a simple exponential specific heat is an order of magnitude greater in lead²⁴ and mercury²⁵ (where the absorption hump is seen) than in other superconductors. The principal objection to this model is the fact that in films as thin as these, scattering is so rapid that we should expect Anderson's theory of dirty superconductors to hold. In this theory, the rapid scattering is treated by replacing the free electron momentum eigenfunctions as starting functions by eigenfunctions for the problem with scattering centers present. Although not defined in detail, these states would *a priori* be expected to be formed with more or less equal weight from all parts of the Fermi energy surface in k space. If this were so, the mixing would average out the anisotropy, leading to an isotropic gap. In this connection, Suhl has recently pointed out²⁶ that if one is considering a case such as, e.g., overlapping s and d bands, then we could have two gaps with a single critical temperature even in the presence of rapid scattering, provided the scattering were such as to conserve the s or d character of the states. It is not clear that this would be the case in practice, however.

The other class of explanation, involving collective effects, is a bit less evident. In Anderson's extension²⁷ of the BCS theory for (pure) superconductors, he shows that under certain conditions it may be possible to produce exciton-like collective excitations with less energy than the minimum required to produce a single-particle excitation at any point on the Fermi surface. These collective excitations may be viewed as analogous to a spin wave. The production of a collective excitation of this type partially excites electrons all over the Fermi surface, instead of completely exciting a single one. The energy of such a collective excited state may be lower than that of the single particle excitation if the interaction matrix element $V_{\mathbf{k}\mathbf{k}'}$ depends strongly on \mathbf{k} and \mathbf{k}' . Even in this case, only a rather specifically prescribed collective excitation can be expected to give the lower energy. These few states could, however, give a large absorption if the coherence required to lower the energy also produced a coherent build up of the transition matrix element. They could not account for any significant effect on the specific heat (in bulk samples) though, because of the small amount of entropy involved. Thus, though the mechanism could explain the observed absorption spectrum, it would not seem to explain the anomalous specific heats of superconducting lead and mercury.

An alternate type of collective excitation has been

²⁴ D. L. Decker, D. E. Mapother, and R. W. Shaw, Phys. Rev. **112**, 1888 (1958).

²⁵ D. K. Finnemore, D. E. Mapother, and R. W. Shaw, Phys. Rev. **118** 127 (1960).

²⁶ H. Suhl, B. T. Matthias, and L. R. Walker, Phys. Rev. Letters, **3**, 552 (1960).

²⁷ P. W. Anderson, Phys. Rev. **112**, 1900 (1958).

²¹ R. W. Morse, T. Olsen, and J. D. Gavenda, Phys. Rev. Letters **3**, 15 (1959).

²² P. W. Anderson, Bull. Am. Phys. Soc. **4**, 148 (1959).

²³ L. N. Cooper, Phys. Rev. Letters **3**, 17 (1959).

tentatively proposed by Ferrell²⁸ and by Stern.²⁹ They note that plasma-like oscillations of the electrons normal to the plane of the film could conceivably be an important mode of motion. Such a mode could be excited by the normal component of the electric field which exists because of the angular width of the incident beam of radiation. Being a resonant mode, it could produce a disproportionately large effect, causing an increase in reflection which would be interpreted (falsely) as an increase in the conductivity in the plane of the film. Preliminary estimates predict that the resonance should occur just above the gap frequency, where it would be relatively difficult to observe. Small changes in the assumed model might lower the resonance to the observed position. Without knowledge of the changes in the model, no definite estimate of intensity is possible. However, it appears likely that the resonance would be unobservably narrow in any case.²⁸ Even if it were the explanation of the structure on the absorption edge, this model would fail to explain the specific heat data.

Summing up, none of the proposed explanations is completely consistent in accounting for all the observed properties. The most promising overall explanation would appear to be one in terms of distinct gaps for separate pieces of Fermi surface, which somehow are not completely averaged out as Anderson's treatment would lead one to expect. Alternatively, one might account for the absorption at the surface or in thin films using Anderson's averaged gap with collective excitations, while accounting for the specific heat results using an anisotropic gap in the more ideal interior of the bulk samples. However, this second approach requires a greater number of distinct assumptions, and it would not explain the apparent *correlation* of nonexponential specific heats with observed structure on the absorption edge.

V. EFFECT OF MAGNETIC FIELD ON LEAD FILMS

The experiment which will be described in this section was actually performed before those mentioned previously. It is more easily understood, however, in the light of the field-free experiments. Lead films were chosen for this work, since lower reduced frequencies could be reached for lead than for other metals.

This experiment was conducted as follows. A lead film was produced in the usual way. The Dewar was then placed between the poles of an electromagnet capable of producing 8000 gauss in the 9-in. gap required for the Dewar. The vacuum system was designed so that the Dewar could be kept evacuated at all times during this moving operation, the diffusion pump being mounted right on the Dewar. After the film was cooled to 1.5°K, the dependence of the critical current I_c upon the field was determined. In the case of Pb1, the

film on which the infrared work was done, the critical current decreased by 2.0% when the field was increased from 0 to 8000 gauss with the field in the plane of the film. In the case of three other films, this decrease in I_c was 4.4%, 5.0%, and 10%, respectively. In all cases, a rotation of the Dewar (and film) in the field in either direction about a vertical axis caused a small additional decrease of I_c , of the order of 1% for a rotation of 3° and 3% for a rotation of 8°, which was the maximum rotation possible, due to space limitations. The field had no measureable effect on the resistance of the film in the normal state.

The effect of the 8000-gauss magnetic field on the infrared properties of Pb1 at 1.5°K was determined as follows. With the film in place and the field off, the strength of the transmission signal was measured at a given frequency. Then the field was turned on and the signal remeasured. This was repeated two or three times, until accurate data had been obtained. The result was a determination of T_0/T_H to within 1% for eleven frequencies between $\hbar\omega/kT_c=2.7$ and 24.9, where T_0 is the transmission through the superconducting film in zero field and T_H is that through the superconducting film in an 8000-gauss field parallel to the film. The data showed that T_0/T_H varied between 1.00 and 1.14, with peaks at 2.7, 4.0 and 8.0 kT_c/\hbar . It was suspected that this strange behavior might be instrumental rather than resulting from properties of the film. This hypothesis was tested by completely oxidizing the film by exposing it to air at room temperature for six hours, causing the film resistance to go to infinity. After this, the dewar was evacuated and cooled to 1.5°K, and the infrared measurements were repeated with the oxidized film. Approximately the same values of T_0/T_H were obtained as with the unoxidized film, indicating that most of the effect of the magnetic field was in fact only instrumental. Further tests at the frequency $4.0kT_c/\hbar$ showed that the change in the signal was approximately proportional to the field. This effect may be due to a dependence of bolometer sensitivity on the field, although this dependence would have to vary non-monotonically with the frequency. Also, the field had no observable effect on the bolometer's dc resistance. Since apparently there was no way to eliminate this effect, an attempt was made to cancel it out by working with the ratio, U , between T_0/T_H for the unoxidized film and that for the oxidized film. The result of these measurements indicated that U was equal to 1.00 to within the random error of 2%, except at the frequencies 4.0 and 5.0 kT_c/\hbar , for which U was 1.04. In view of possible systematic errors, it is not certain that the field had any significant effect on the film, even at these two frequencies. (The frequency dependence of T_S/T_N was also determined for the same lead film, Pb1. Because of improvements in technique which were made after this film was run, data are less accurate than those obtained with Pb2

²⁸ R. A. Ferrell (private communication).

²⁹ E. A. Stern (private communication).

and Pb3. The shape of the T_S/T_N curve for Pb1 was approximately the same as that of Pb3, however.)

In interpreting the infrared results, one might consider changes in the gap width and in the low frequency supercurrent response σ_2^A . One might expect a magnetic field to decrease the size of the gap. The effect of this would be a shift of the curve to lower frequencies. The smallness of the observed effect of the 8000 gauss field on the ratio U indicates that any shift of the curve is by less than 2%. The fact that $U=1.04$ for $\hbar\omega/kT_c=4$ and 5, if significant, probably means that the gap edge is smeared out by the field.

If the field had affected σ_2^A/σ_N , the low-frequency values of U would have also been affected. From the smallness of the effect of the field on U , it is apparent that σ_2^A/σ_N was altered by less than 2% by the field. The low-frequency penetration depth, which is proportional to $(\sigma_2^A)^{-\frac{1}{2}}$, was therefore affected by less than 1% by the field.

The two most precise experiments with which these findings can be compared are those of Pippard³⁰ and of Spiewak.³¹ Working with tin wires in a transverse static magnetic field, Pippard showed that the behavior of his samples in a microwave field of frequency 9.4 kMc/sec indicated that the superconducting penetration depth was increased by the static field. This increase was less than 3% for a magnetic field almost equal to the critical field of the wire (about 300 gauss) when the sample was at a temperature low compared with the critical temperature. Spiewak's experiments were performed with oriented single-crystal tin wires in both transverse and longitudinal static magnetic fields, at a frequency of 1.0 kMc/sec. Her results also indicate that the magnetic field has a very small effect on the superconducting sample. For instance, the application of a longitudinal field equal to 0.9 times the critical field changed the surface reactance by less than 1% of the change caused by increasing the field above the critical field to make the sample become normal. (The surface reactance is approximately proportional to the penetration depth in the superconducting state if the temperature is low compared with the critical temperature.) Our results may be compared with those of Pippard and of Spiewak by noting that $\sigma_2^A(\omega)$ is inversely proportional to the square of the low-frequency penetration depth in a bulk sample.

It might be advantageous in comparing these experiments to know the critical field of the film used. There were no facilities available for obtaining fields high enough to determine this, but an extrapolation of the

data obtained by Appleyard, Bristow, London, and Misener³² for mercury films, or those obtained by Alekseyevski³³ for tin films suggests that a lead film about 12 Å thick would have a critical field of at least 25 000 gauss.

Unfortunately, there have been no theoretical calculations performed on the basis of the BCS theory with which the data described in this section could be compared.

VI. SUMMARY OF CONCLUSIONS

The transmission of infrared radiation for wavelengths between 0.1 and 1.1 mm through superconducting films of lead, tin, indium, and mercury has been measured. The transmission data have been analyzed to find the ratio of the conductivity in the superconducting state to that in the normal state. The following are the main conclusions of this analysis.

The values obtained for the width of the energy gap divided by kT_c are approximately equal to the value 3.5 predicted by BCS, but are in somewhat better agreement with both calorimetric and far infrared experiments on bulk samples than with the theory. The frequency dependence of the conductivity ratio is in semiquantitative agreement with the calculation of Mattis and Bardeen, which is based on the BCS theory. However, $\sigma_1(\omega)/\sigma_N(\omega)$ rises somewhat more steeply above the gap, and approaches unity more rapidly than predicted. In the case of lead and (tentatively) mercury, a low-frequency hump in the $\sigma_1(\omega)/\sigma_N(\omega)$ curve has been observed which was not predicted by Mattis and Bardeen, but which may be due to collective excitations as described by Anderson and by Ferrell and Stern, or to an anisotropy in the energy gap. The magnitude of the imaginary part of the reduced superconducting conductivity ratio at low frequencies, $\sigma_2^A(\omega)/\sigma_N(\omega)$, is in reasonable agreement both with the BCS theory and with microwave measurements. Finally, it has been determined that a magnetic field as large as 8000 gauss has no reliably observable effect on the transmissivity of a lead film about 12 Å thick. This seems compatible with the results of microwave experiments on bulk tin.

VII. ACKNOWLEDGMENTS

The authors gratefully acknowledge the assistance of Dr. R. E. Glover, III, in designing the Dewar used in these experiments. Thanks are also due to P. L. Richards for cooperation in the design and construction of the far infrared monochromator.

³⁰ A. B. Pippard, Proc. Roy. Soc. (London) **A203**, 210 (1950).

³¹ M. Spiewak, Phys. Rev. **113**, 1479 (1959).

³² E. T. S. Appleyard, J. R. Bristow, H. London, and A. D. Misener, Proc. Roy. Soc. (London) **A172**, 540 (1939).

³³ N. E. Alekseyevski, J. Phys. (U.S.S.R.) **4**, 401 (1941).